Journal of Engineering Research (JER)
ISSN: 2356-9441 Vol. 8 – No. 4, 2024 ©Tanta University, Faculty of Engineering e ISSN: 2735-4873

The Effect of Road Profile on the Performance of a Full Car Suspension Model Ride Comfort

Bassem Nashaat Zakher [1,*], Ibrahim M. El Fahham [1,2], M. Elhadary [2], M. El-Gohary [2,3]

[1] Faculty of Industrial and Energy Technology, Borg Alarab Technological University, Egypt.

[2] Mechanical Engineering Department, Faculty of Engineering, Alexandria University, Egypt.

[3] Mechanical Engineering Department, Faculty of Engineering, Beirut Arab University, Lebanon

*Corresponding author's email: bassem.zakher1@gmail.com

***Abstract*- A full-car eight degrees of freedom model is used to investigate the dynamic response of vehicles subjected to different road profiles on ride comfort. Two road profiles are used in this study that includes the effect of the vehicle mass and moment of inertia on the vehicle ride comfort. In the proposed vehicle model, the masses of the tires, damping and stiffness are variables. Also, the suspensions parameters and the location of the centre of gravity of the vehicle body can be changed. Lumped Mechanical System interface of COMSOL Multiphysics is used to model the tires, the suspension system as well as the seats with a passenger using mass, spring, and damper nodes. The vehicle chassis is modelled as a rigid body with three degrees of freedom in the multi-body dynamics interface. A transient analysis is performed to compute the vehicle motion as well as the seat vibration levels for a given road profile. It was found that the displacement and pitch angular velocity of vehicle C.G. and front left seat are higher under rectangular road bump profile than in sinusoidal road profile. On the other hand, the front left seat acceleration and jerk analysis shows that rectangular road profile have also higher values than sinusoidal road profile. The recording uncomfortable condition in accordance to the ISO standard. In continuous irregular road profile however, the values recorded for rectangular bump are lower in single bump for both acceleration and jerk. Whereas for continuous sinusoidal bumps extreme values of acceleration and jerk were recorded.**

***Keywords*- Car suspension, dynamic response, multibody dynamics, passive seat suspensions, road profile**

INTRODUCTION

A vehicle development program needs the full car specified data that reflects the simulation operating conditions. A designer's adjustments are simpler and less expensive in the early phases of the design process than they are in the latter stages when they become quite expensive. Research is now being done on how to anticipate the load operating on the entire vehicle using road profiles and vehicle models. In such research programs, a vital element in is the ability to identify the road profile precisely.

The irregularity of the road surface is the main cause of vibration in the vehicle. Presently, the synthetic type bumps are used in city areas, which are more dangerous for human health, as vehicle body acceleration is very high. Vibration plays a crucial part in ride comfort, vehicle safety, and overall vehicle performance. Vehicle dynamic analysis has been a popular research area for many years.

There have been several publications that include theoretical and experimental research on the dynamic behavior of passively and actively suspended road vehicles. The development of the quarter-car model, half-car model, and full-vehicle model was based on studies of the dynamics of the vehicle and the management of vibration. Although mathematical modelling tools for analysis/computation have grown tremendously, most vehicle dynamics research are based on the assumption that all vehicle system parameters are deterministic. Actually, due to manufacturing tolerances and/or wear, ageing, and so on, the spring stiffness and damping rate may differ from the nominal value. Due to the variety of possible vehicle loading conditions and the uncertainty of the inflating pressure of poorly maintained tires, the vehicle body mass and tire radial stiffness can exhibit stochastic variations. Weight and passenger placements vary significantly in cars and buses. Furthermore, even vehicles of the same brand and type leaving the assembly line may have differences in size, mass, performance.

Passive seat suspensions have long demonstrated that they are suboptimal single degree of freedom (SDOF) suspension systems. Once the spring rate has been chosen, thus setting the natural frequency, the other parameter that needs to be chosen is the system damping. Insufficient damping provides poor resonance control, but good isolation at high frequencies. Conversely, large damping results in good resonance control while

sacrificing high frequency isolation. In the realm of enhancing ride quality, stability, and overall handling of vehicles, suspension systems play an indispensable role. One such vital component is the passive suspension system, which operates using straightforward yet highly effective mechanisms to ensure a comfortable and well-controlled ride. It is worth gaining insight into their functionality and the merits they bring to the automotive industry.

Fayyad "et al.,". [1], As the name implies, passive suspension systems function without the need for active control or external power sources. These systems typically encompass hydraulic or mechanical elements, including springs, shock absorbers, and various linkage components. The central objective of a passive suspension system is to guarantee that a vehicle's wheels remain in consistent contact with the road surface, even when navigating uneven or rough terrains.

Advantages of passive suspension systems are cost-effective since active ones necessitate electronic components and sensors. Passive systems are also mechanically less complex and possess fewer components susceptible to malfunction, resulting in enhanced reliability and simplified maintenance. This makes passive suspension an appealing choice for many vehicle manufacturers and consumers. On the other hand, active suspension systems rely on real-time data which provide better road feedback, leading to improved handling and a more engaging driving experience.

Dynamic tire loading was studied by Valesek "et al.," [2]. These studies looked into ways to lessen a vehicle's dynamic tire loading in an effort to lessen the amount of road damage it produces. Three further experiments concentrated on control strategies that might instruct themselves how to manage the semiactive suspension system.

MA El-Gohary "et al.," [3], utilizing electronic sensing, communication, and computation technologies to regulate vehicle movement on restricted access highways is known as highway automation. When a car is fully automated, the driver just has to provide direction when choosing the route from point A to point B and input to the emergency systems. The car's braking, steering, and throttle are entirely computer controlled while it is driving on a highway.

S Yaghoubi "et al.," [4]. Concluded that in order to reduce the amount of vehicle vibration the current MR dampers have been added to the one-half car model (for both wheels of the simulated model) with four degrees of freedom, and the effects of improving the performance of the suspension system have been researched. In order to model the vehicle system, the particle swarm optimization (PSO) algorithm is applied with the aim of extracting the optimal values of the suspension system parameters and checking the amount of reduction in vehicle vibrations. Two optimization modes were considered. In the first case, the parameters of the suspension system were assumed to be fixed, and only the optimization of the MR damper variables was done. In the second case, the amount of the objective function is obtained based on the optimization of all the variables of the suspension system.

Mahmoud El-Kafafy "et al.," [5], proposed a two degree of freedom quarter vehicle which is used to study the performance of magneto-rheological (MR) fluid dampers of the Bouc-Wen type in automotive ride comfort. The MR damper is forced to obey the dynamics of the ideal sky-hock model using the sliding mode control. Two excitations are used to test the model, a road hump with a high peak amplitude and a statistically random road. Using Matlab/Simulink software, the results are created and displayed in the time and frequency domains. Root mean square values are used for comparison with fully active, ideal semi-active, and conventional passive suspension systems. The adjustable MR damper offers a significant improvement for the vehicle road, according to simulation findings for the developed controller.

L Batistini "et al.," [6], proposed a relatively simple model to compute the loads on the suspension arms and at the tires' contact patches of a Formula SAE car. The model is based on standard dynamic equilibrium equations, a simplified assumption for the limited-slip differential, and a given front-to-rear brake distribution. The model inputs are the signals acquired with common telemetry sensors, which usually equip a Formula SAE vehicle. To validate the model, some arms of the suspensions were instrumented with strain gauges, and a kinematic model of the suspension, together with its static equilibrium equation set, was set up to relate the arm loads to the forces acting at the tire-road contact patch. The kinematic and equilibrium of suspension models were first validated through static tests with known forces applied at the wheel hub. Then, the complete vehicle model was validated by comparing the same quantities relative to some real driving tests on a kart circuit, showing a fairly good agreement between the predicted and measured loads.

J Kumar "et al.," [7], enhance ride comfort and vehicle stability by using long-term vibration from an uneven road surface has an impact on rider comfort, safety, and health in addition to the vehicle's stability. Conventional MR suspension reduces vibration energy but cannot avoid the resonance between the excitation and the vehicle without stiffness control. This results in the proposal of a novel hybrid vibration isolator with tunable stiffness and damping. Isolator produces independent variable stiffness and independent variable damping characteristics, respectively, by combining magneto-rheological (MR) fluid with MR elastomer. The two road profiles that are thought to supply input to the suggested system are sinusoidal and random.

AE Geweda "et al.," [8], develops a seven degrees of freedom whole vehicle MATLAB SIMULINK model, by applying the ideas of the free body diagram and Newton's second law, mathematical equations can be found. To make sure the SIMULINK model is appropriate for researching ride comfort, validation of the model is acquired. The front and rear passive

suspension systems of the seven DOF vehicle model are optimized for spring stiffness and damping coefficient at different velocities using a genetic algorithm optimization technique. This improves the vehicle's suspension system performance.
MP Nagarkar "et al.," [9], The modeling and optimization of the quarter car suspension system employing the Macpherson strut is presented in this study. Using the MATLAB/Simulink environment, a mathematical model of a quarter vehicle is created, simulated, and optimized. Test rigs are used to validate the results. A genetic algorithm is used to optimize the suspension system parameters for the following objective functions, maximum transient vibration value, frequency weighted root means square acceleration (also known as RMS acceleration), vibration dose value (VDV), root mean square suspension space, and root mean square tire deflection. The ISO 2631-1 standard is used to evaluate the ride and health requirements. The results indicate that, in comparison to classical design, the ideal parameters offer ride comfort and health criteria.
MF Yakhni "et al.," [10], design the optimum suspension system to provide ride comfort and handling ability in all driving conditions has become a significant and demanding responsibility for automakers. They offer support for improving the suspension system's efficacy. Using MATLAB/Simulink, a complete automobile model with eight Degrees of Freedom (DOF) was created. The Simulink model was found to be validated. It was predicted that the model will traverse a half-sine wave-shaped speed hump with an amplitude varying from 0.01 to 0.2 meters.
A Abd_Elsalam "et al.," [11], examines the nonlinear quarter car suspension system's simulation reactions while the vehicle rides over a model bump that is simulated to act as a road excitation. The primary goal of the current effort is to thoroughly show a front quarter automobile suspension model in order to examine how the suspension system behaves when moving over a bump. The simulation program MATLAB/SIMULINK is used to model the traditional suspension system. The suspension system design dependence on the chosen bump form can be tested by the designer thanks to the model.
ANSZ Abidin """"et al.," [12], look at the current state of street crash information collection and administration in ASEAN's middle-income level nations by proceeding to utilize the "3-5-2" concept borrowed from past papers. Talking about the plausibility of turning the 'Midfields' into forwards by watching patterns of information where encourage enhancement can be executed utilizing high-income nations as reference.
Bassem Nashaat Zakher ""et al.," [13], investigated how the interaction of a fluid with a structure is an important phenomenon, particularly the interaction between a dynamic vehicle and the airflow. Computational fluid dynamics and Fluid-structure interaction models are developed to simulate the performance of a sedan car. Also, an experimental live road simulation is conducted for a Skoda Octavia A4 sedan car to validate the performance and the accuracy of the presented models at cruising speeds between 40 to 100 km/hr. Where the results show that the aerodynamic forces have a minor effect on the displacement, pitching angle, transverse velocity, and transverse acceleration at the range of low cruise speeds of about 36 km/hr. on the other hand, the effect of road profile on vehicle dynamic parameters resulted in this cruise speed of 36 km/hr which indicates that the dynamic simulation has a great effect on car performance at low cruise speeds.
Ksander N. de Winkel "et al.," [14], investigated that discomfort increases with acceleration amplitude and that the strength of this effect depends on the direction of motion. In addition, it was found that higher jerks (shorter duration pulses) are considered more comfortable, and that triangular pulses are more comfortable than sinusoidal pulses, in addition a novel statistical model that describes motion comfort as a function of acceleration, jerk, and direction was concluded. The outputs were essential to develop motion planning algorithms aimed at maximizing comfort.

The main aim of this work is to develop a passive suspension for a passenger car using a full car model (eight degree of freedom) in a lumped mechanical system interface of COMSOL Multiphysics. This simulation model is used as a platform to analyze the performance of vehicle dynamics response and interactions with aerodynamic (Fluid-structure interaction) and its effect on passenger ride comfort for different standard road profiles.

I. Methodology

The suspension system used on a car wheel is the basis of the model being developed in this work with finite element method using COMSOL software. The main system components are:
1-Vehicle eight degree of freedom full car model
2-Equations of motion for a vehicle suspension, chassis and driver's seat.
3-Vehicle parameters.
4-Road excitation.

A. Vehicle suspension system model

Figure. 1 depicts the non-linear whole automobile model that was employed in this investigation. It incorporates every conceivable control method. The eight degrees of freedom in this whole car model are (Z_{u1}, Z_{u2}, Z_{u3}, Z_{u4}, Z_{u5}, Z, θ and Φ).
These are, respectively, the motion of the passenger seat, the motion of the vehicle body, the pitch motion of the vehicle body, and the roll motion of the vehicle body. They also include the motion of the right front axle, the motion of the left front axle, the motion of the right rear axle, the motion of the left rear axle, the motion of the passenger seat, and the motion

Journal of Engineering Research (JER)
ISSN: 2356-9441 Vol. 8 – No. 4, 2024 ©Tanta University, Faculty of Engineering e ISSN: 2735-4873

of the vehicle body, the goal is to make the guests' rides more comfortable.

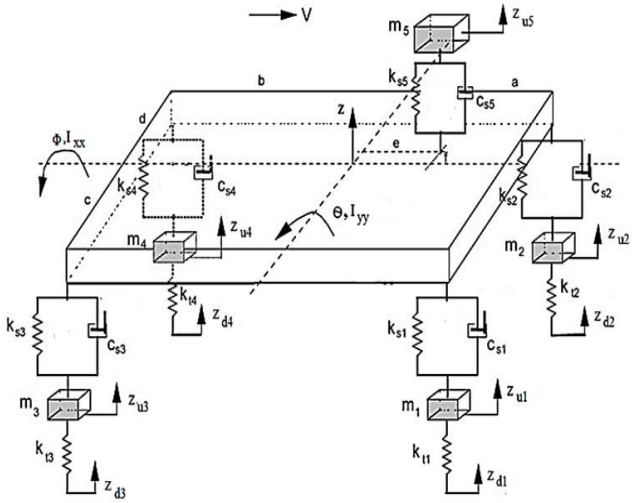

Figure. 1- The non-linear full car model with a passenger seat [15]

B. Equations of motion for a vehicle suspension syste

Eq. (1) represents the equation of motion for heave at center of gravity of vehicle, eq. (2) represents the motion for pitch at center of gravity around (Y-axis) clockwise, eq. (3) represents the motion for roll at center of gravity around (X-axis) clockwise, in addition eq. (4) represents the motion for (front – right) unsprung mass, eq. (5) represents the motion for (front – left) unsprung mass, on the other hand eq. (6) represents the motion for (rear-right unsprung mass while eq. (7) represents the motion for (rear – left) unsprung mass, finally eq. (8) represents the motion for the seat mass [18].

$$
\begin{aligned}
M\ddot{Z} = {} & K_{s1}Z_{u1} + K_{s2}Z_{u2} + K_{s3}Z_{u3} + K_{s4}Z_{u4} + K_{s5}Z_{u5} \\
& - [K_{s1} + K_{s2} + K_{s3} + K_{s4} + K_{s5}]Z \\
& - [a(K_{s1} + K_{s2}) - b(K_{s3} + K_{s4}) + eK_{s5}]\Theta \\
& - [d(K_{s2} + K_{s4}) - c(K_{s1} + K_{s3}) + fK_{s5}]\Phi \\
& + C_{s1}\dot{Z_{u1}} + C_{s2}\dot{Z_{u2}} + C_{s3}\dot{Z_{u3}} + C_{s4}\dot{Z_{u4}} \\
& + C_{s5}\dot{Z_{u5}} - [C_{s1} + C_{s2} + C_{s3} + C_{s4} + C_{s5}]\dot{Z} \\
& - [a(C_{s1} + C_{s2}) - b(C_{s3} + C_{s4}) + eC_{s5}]\dot{\Theta} \\
& - [d(C_{s2} + C_{s4}) - c(C_{s1} + C_{s3}) \\
& + fC_{s5}]\dot{\Phi} \qquad (1)
\end{aligned}
$$

$$
\begin{aligned}
& I_{yy}\ddot{\Theta} \\
& = aK_{s1}Z_{u1} + aK_{s2}Z_{u2} - bK_{s3}Z_{u3} - bK_{s4}Z_{u4} + eK_{s5}Z_{u5} \\
& - [a(K_{s1} + K_{s2}) - b(K_{s3} + K_{s4}) + eK_{s5}]Z \\
& - [a^2(K_{s1} + K_{s2}) + b^2(K_{s3} + K_{s4}) + e^2K_{s5}]\Theta \\
& - [d(aK_{s2} - bK_{s4}) - c(aK_{s1} - bK_{s3}) + efK_{s5}]\Phi \\
& - [a(C_{s1} + C_{s2}) - b(C_{s3} + C_{s4}) + eC_{s5}]\dot{Z} \\
& - [a^2(C_{s1} + C_{s2}) + b^2(C_{s3} + C_{s4}) + e^2C_{s5}]\dot{\Theta} \\
& - [d(aC_{s2} - bC_{s4}) - c(aC_{s1} - bC_{s3}) + efC_{s5}]\dot{\Phi} \\
& + aC_{s1}\dot{Z_{u1}} + aC_{s2}\dot{Z_{u2}} - bC_{s3}\dot{Z_{u3}} - bC_{s4}\dot{Z_{u4}} \\
& + eC_{s5}\dot{Z_{u5}} \qquad (2)
\end{aligned}
$$

$$
\begin{aligned}
& I_{xx}\ddot{\Phi} \\
& = -cK_{s1}Z_{u1} + dK_{s2}Z_{u2} - cK_{s3}Z_{u3} + dK_{s4}Z_{u4} + fK_{s5}Z_{u5} \\
& - [d(K_{s2} + K_{s4}) - c(K_{s1} + K_{s3}) + fK_{s5}]Z \\
& - [d^2(K_{s1} + K_{s2}) + c^2(K_{s3} + K_{s4}) + f^2K_{s5}]\Phi \\
& - [d(aK_{s2} - bK_{s4}) - c(aK_{s1} - bK_{s3}) + efK_{s5}]\Theta \\
& - [d(C_{s2} + C_{s4}) - b(C_{s1} + C_{s3}) + fC_{s5}]\dot{Z} \\
& - [d^2(C_{s2} + C_{s4}) + c^2(C_{s1} + C_{s3}) + f^2C_{s5}]\dot{\Phi} \\
& - [d(aC_{s2} - bC_{s4}) - c(aC_{s1} - bC_{s3}) + efC_{s5}]\dot{\Theta} - cC_{s1}\dot{Z_{u1}} \\
& + dC_{s2}\dot{Z_{u2}} - cC_{s3}\dot{Z_{u3}} + dC_{s4}\dot{Z_{u4}} \\
& + fC_{s5}\dot{Z_{u5}} \qquad (3)
\end{aligned}
$$

$$
m_1\ddot{Z_{u1}} = -(K_{s1} + K_{t1})Z_{u1} + K_{s1}Z + aK_{s1}\Theta - cK_{s1}\Phi - C_{s1}\dot{Z_{u1}} + C_{s1}\dot{Z} + aC_{s1}\dot{\Theta} - cC_{s1}\dot{\Phi} + K_{t1}Z_{d1} \qquad (4)
$$

$$
m_2\ddot{Z_{u2}} = -(K_{s2} + K_{t2})Z_{u2} + K_{s2}Z + bK_{s1}\Theta + dK_{s1}\Phi - C_{s2}\dot{Z_{u2}} + C_{s2}\dot{Z} + bC_{s1}\dot{\Theta} + dC_{s1}\dot{\Phi} + K_{t2}Z_{d2} \qquad (5)
$$

$$
m_3\ddot{Z_{u3}} = -(K_{s3} + K_{t3})Z_{u1} + K_{s3}Z - bK_{s3}\Theta - cK_{s3}\Phi - C_{s3}\dot{Z_{u3}} + C_{s3}\dot{Z} - bC_{s3}\dot{\Theta} - cC_{s3}\dot{\Phi} + K_{t3}Z_{d3} \qquad (6)
$$

$$
\begin{aligned}
& m_4\ddot{Z_{u4}} \\
& = -(K_{s4} + K_{t4})Z_{u4} + K_{s4}Z - bK_{s4}\Theta + dK_{s4}\Phi - C_{s4}\dot{Z_{u4}} \\
& + C_{s4}\dot{Z} - bC_{s4}\dot{\Theta} + dC_{s4}\dot{\Phi} \\
& + K_{t4}Z_{d4} \qquad (7)
\end{aligned}
$$

$$
m_5\ddot{Z_{u5}} = -K_{s5}Z_{u5} + K_{s5}Z + eK_{s5}\Theta + fK_{s5}\Phi - C_{s5}\dot{Z_{u5}} + C_{s5}\dot{Z} + eC_{s5}\dot{\Theta} + fC_{s5}\dot{\Phi} \qquad (8)
$$

C. Full car vehicle model parameters

Figure. 2 shows the overall dimensions of the car used in this analysis. As a lumped parameter model approach is used in this analysis, the actual geometry of the system is

Journal of Engineering Research (JER)
ISSN: 2356-9441 Vol. 8 – No. 4, 2024 ©Tanta University, Faculty of Engineering e ISSN: 2735-4873

not required and simplified model geometry based on the overall dimensions is considered for this, Figure. 3 describes the details for tire, wheel and Seat Subsystem, Figure. 4 illustrate a simplified full-car vehicle model with passive suspension system. In addition, Table 1 lists the system
parameters used to model full-car vehicle and passive suspension system.

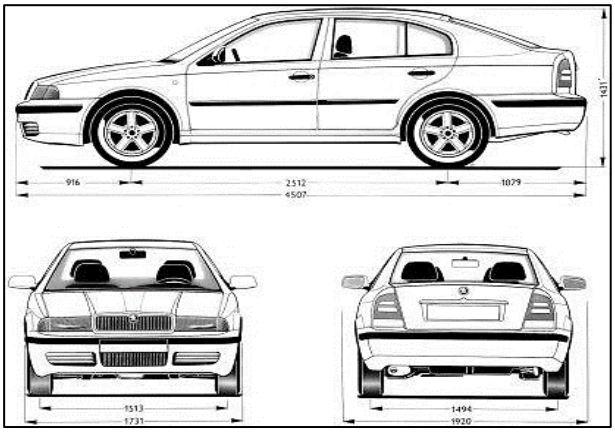

Figure. 2- Overall dimensions of the car

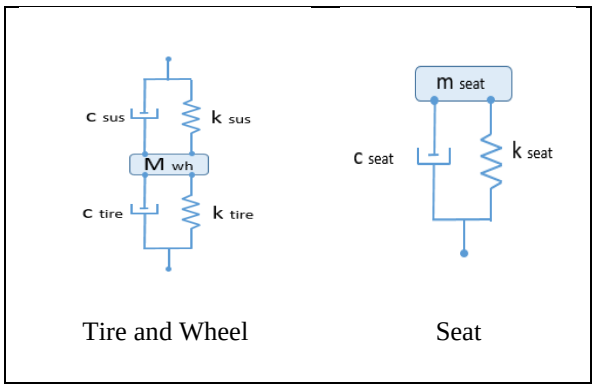

Figure. 3- Tire Wheel and Seat Subsystem Details

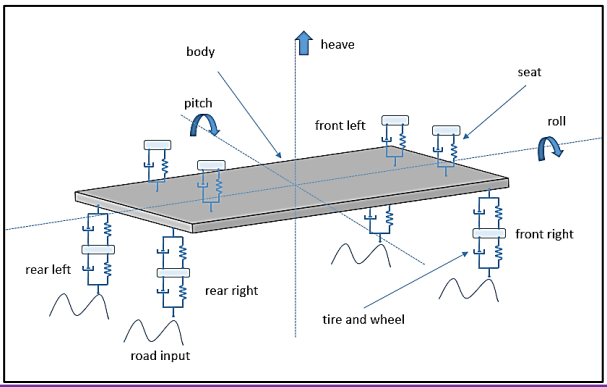

Figure. 4- Simplified full-car vehicle model with passive suspension system

Table 1 - System parameters used to model full-car vehicle and passive suspension system [13]

Name	Value	Description
m_body	1800 kg	Mass of vehicle body
r_wb	2.512 m	Wheelbase (Distance between two axles)
r_tw	1.513 m	Track width (Distance between two wheels of the same axle)
a	1.256 m	longitudinal distance of the tire from CG
b	0.7565 m	lateral distance of the tire from CG
I_roll	1030.1 kg·m²	Inertia around roll
I_pitch	2839.6 kg·m²	Inertia around pitch
m_p	120 kg	Mass of passengers with seat
k_seat	1750 N/m	Stiffness of seat springs
c_seat	700 N·s/m	Damping of seat dampers
k_sus	18000 N/m	Stiffness of suspension springs
c_sus	1400 N·s/m	Damping of suspension dampers
m_wh	60 kg	Mass of wheels (Unsprung mass)
k_tyre	180000 N/m	Stiffness of wheels (Tire stiffness)
c_tyre	700 N·s/m	Damping of the wheel (Tire damping)
hb	0.05 m	Bump height
wb	0.4 m	Bump width
speed	10 m/s	Vehicle speed
tb	0.16 s	Bump time period
td	0.2512 s	Time delay between front and rear wheel

Table 2- The ISO 2631-1 standard defines six levels of ride comfort [14]

Comfort level	Acceleration m/s²	Comfort level	Acceleration m/s²
comfortable	≤ 0.315	uncomfortable	0.80 to 1.60
slightly uncomfortable	0.315 to 0.63	very uncomfortable	1.25 to 2.00
quite uncomfortable	0.50 to 1.00	Extremely uncomfortable	> 2.00

D. Road profiles

The cruising speed used in simulation (36 km/hr) is based on the actual passenger comfort driving speed when passing over irregular road profile conducted with bumps. In

Journal of Engineering Research (JER)
ISSN: 2356-9441 Vol. 8 – No. 4, 2024 ©Tanta University, Faculty of Engineering e ISSN: 2735-4873

addition, this cruise speed is concluded from an experimental live road simulation [13], where the results shows that the aerodynamic forces have a minor effect on the displacement, pitching angle, transverse velocity and transverse acceleration at the range of low cruise speeds about 36 km/hr. The effect of road profile on vehicle dynamic parameters are clearly resulted for this cruise speed 36 km/hr which indicates that the dynamic simulation has the great effect on car performance at low cruise speeds. On the other hand, it is recommended for simulations at low cruise speeds below 36 km/hr where the deformation of mesh does not occur (no interaction) we can use the dynamic model simulation which can save time and effort, but for the other cruise speeds we have to take in account the effect of aerodynamic forces with the presence of FSI model.

E. Single pulse road excitation profiles

Two different road profiles are modelled in this analysis for comparison purposes. Figure. 5& 6 illustrates a rectangular bump and a sinusoidal bump. A special case of the vehicle passing over the bump with a speed of 36 km/hr is considered here. Only the left side of the vehicle (front and rear wheels of the left side of the vehicle) are considered as passing over the bump.

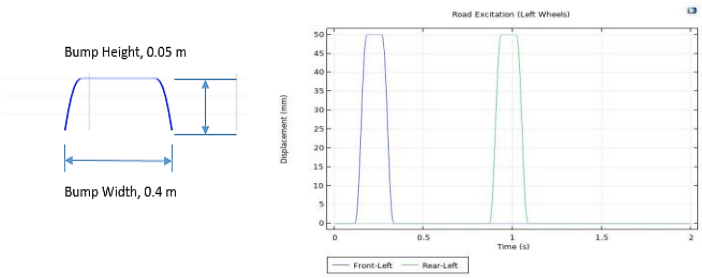

Figure. 5 - Rectangular Pulse Road Profile

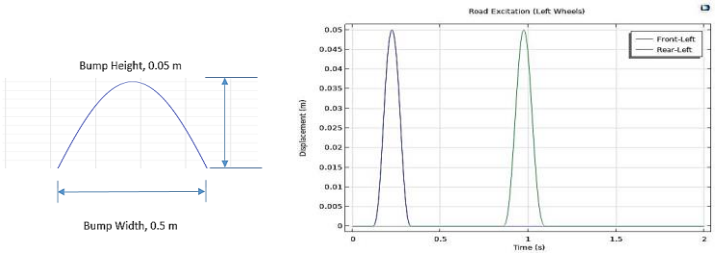

Figure. 6 – Sine Pulse Road Profile

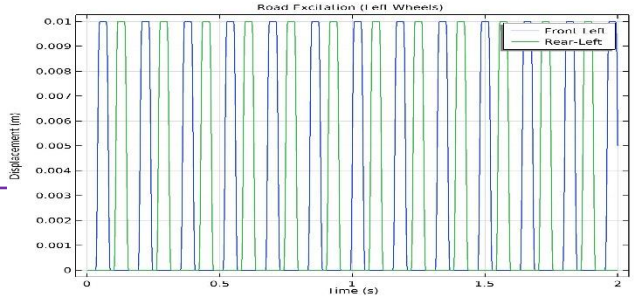

Figure. 7– continuous rectangular road profile

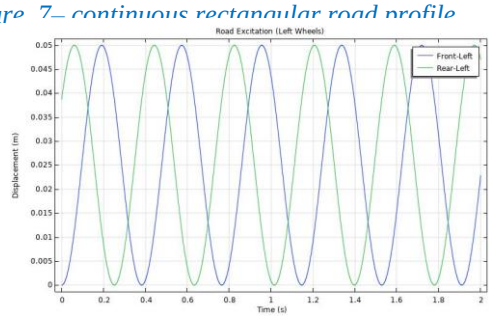

Figure. 8– continuous sinusoidal road profile.

II. Results and discussion

Using the COMSOL Multiphysics simulation model, Figure. (9) presents the angular rotation at car CG for rectangular and sinusoidal bump road profiles. Figure. (10) presents the heave displacement at the centre of gravity for rectangular and sinusoidal bump road profiles. Whereas the angular velocity at the centre of gravity between the rectangular and sinusoidal bumps is shown in Figure. (11). The heave velocity has a peak value of 0.06 m/sec for rectangular bumps and 0.055 m/sec for sinusoidal bumps as shown in Figure. (12) and Figure. (13) illustrates this comparison. In addition, Figure. (14) shows the comparison between the seat acceleration of the model for both wheels regarding the two road profiles used. Figure. (15) illustrates the spring forces and damping forces at the front left wheelbase, finally Figure. 16) presents the comparison between the forces at the front seat on the left side for both rec and sinusoidal road profiles.

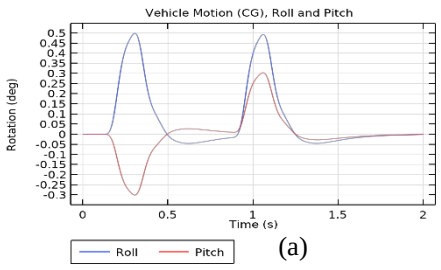

(a)

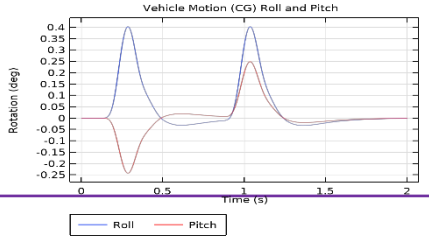

Figure. 9 – Rotation at the centre of gravity, roll and pitch
(a) For Rectangular Bump, (b) Sinusoidal Bump

(b)

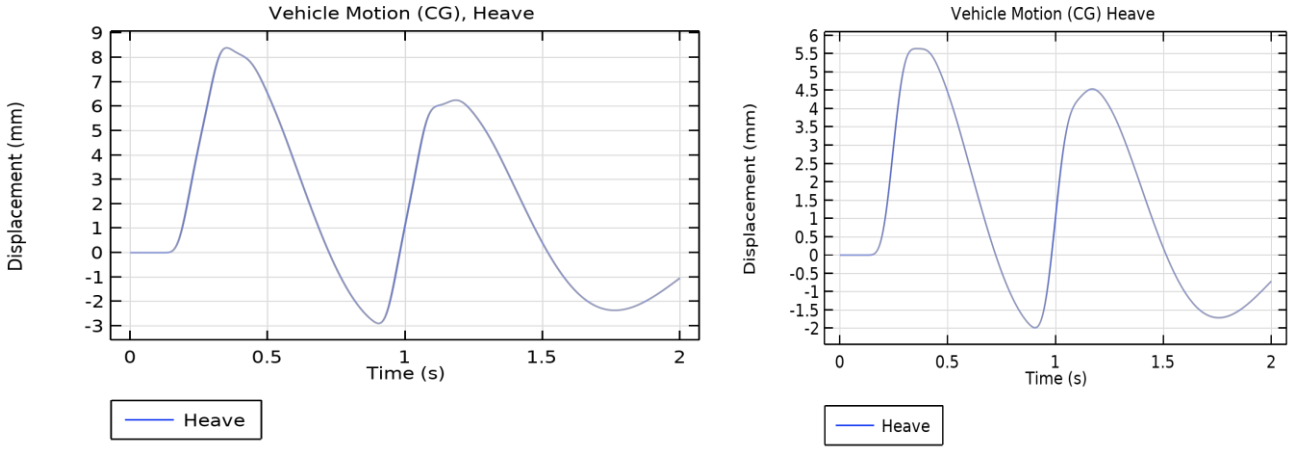

(a) *(b)*

Figure. 10 – Heave displacement at the centre of gravity, Heave
(a) For Rectangular Bump, (b) Sinusoidal Bump

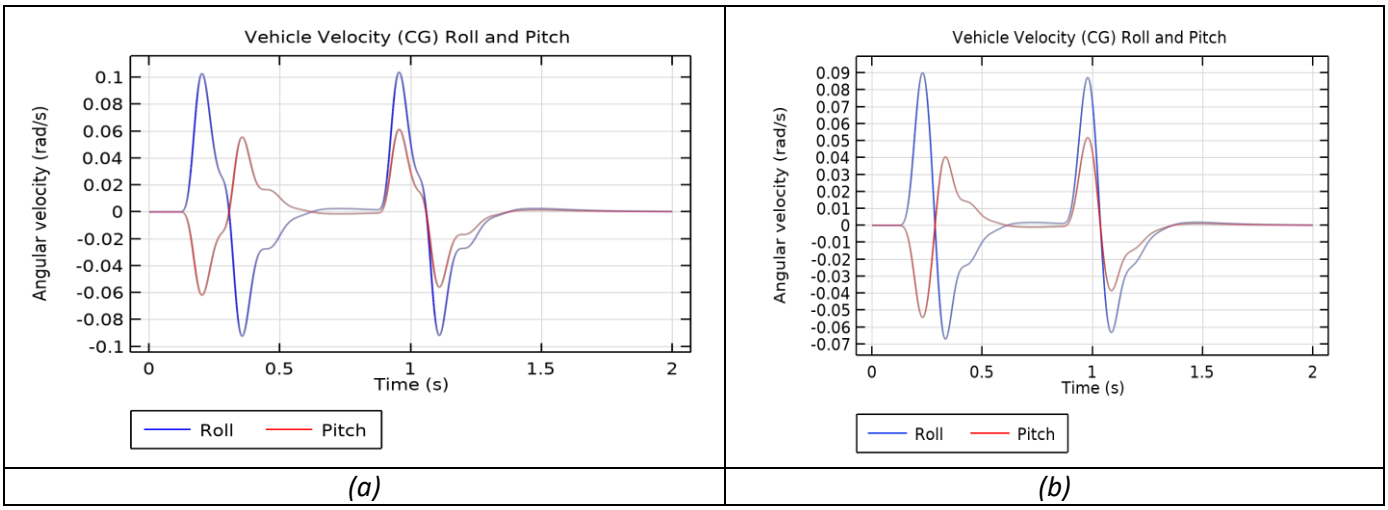

(a) *(b)*

Figure. 11 – Angular Velocity at the centre of gravity, roll and pitch
(a) For Rectangular Bump, (b) Sinusoidal Bump

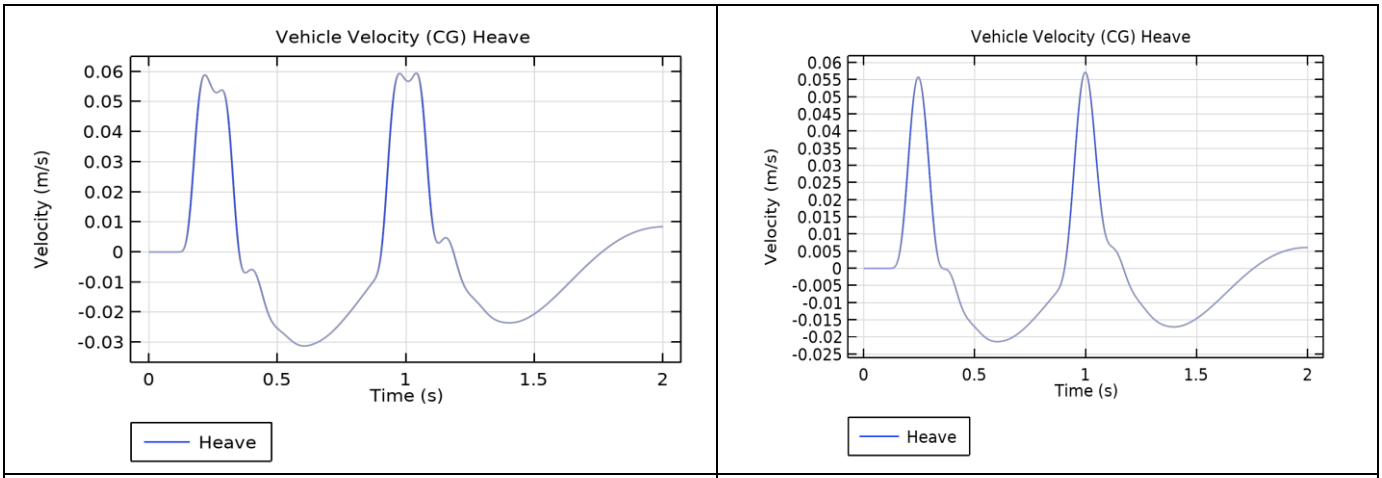

(a) *(b)*

Figure. 12 –Heave velocity at the centre of gravity
(a) For Rectangular Bump, (b) Sinusoidal Bump

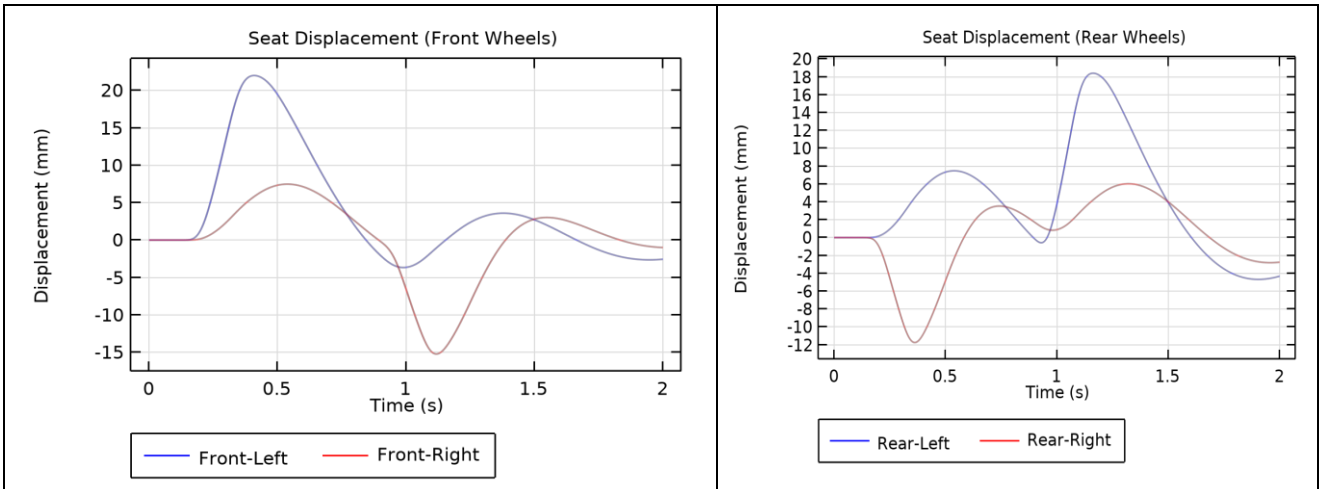

(1) *(2)*

(a) Rectangular Bump

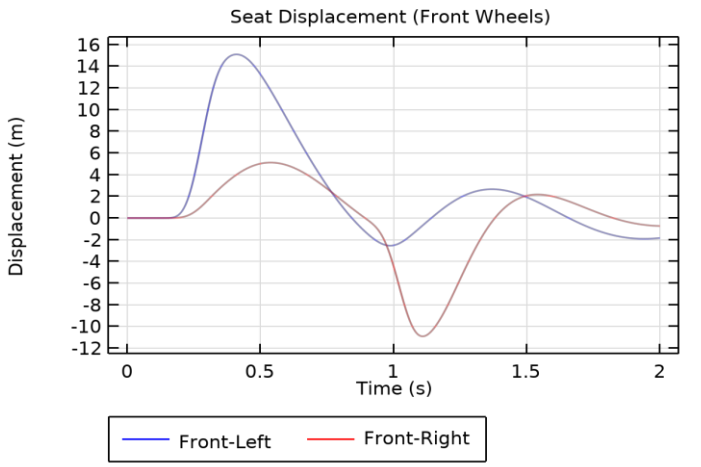

(3)

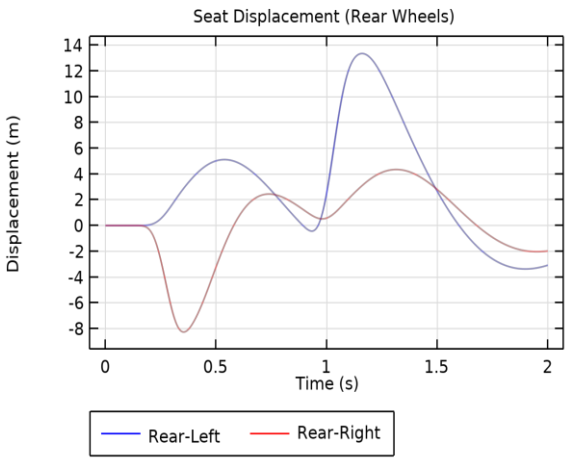

(4)

(b) Sinusoidal Bump

Figure. 13 - Seat displacement of the model
(a) Rectangular Bump, (b) Sinusoidal Bump

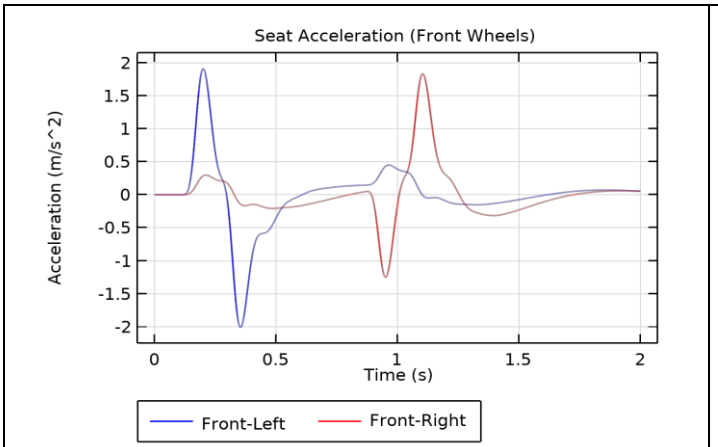

(1)

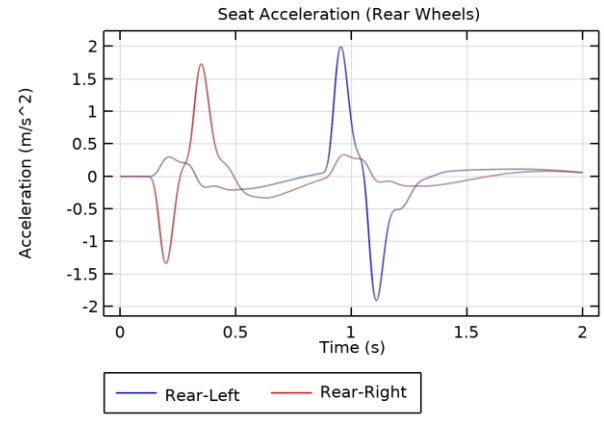

(2)

(a) Rectangular Bump

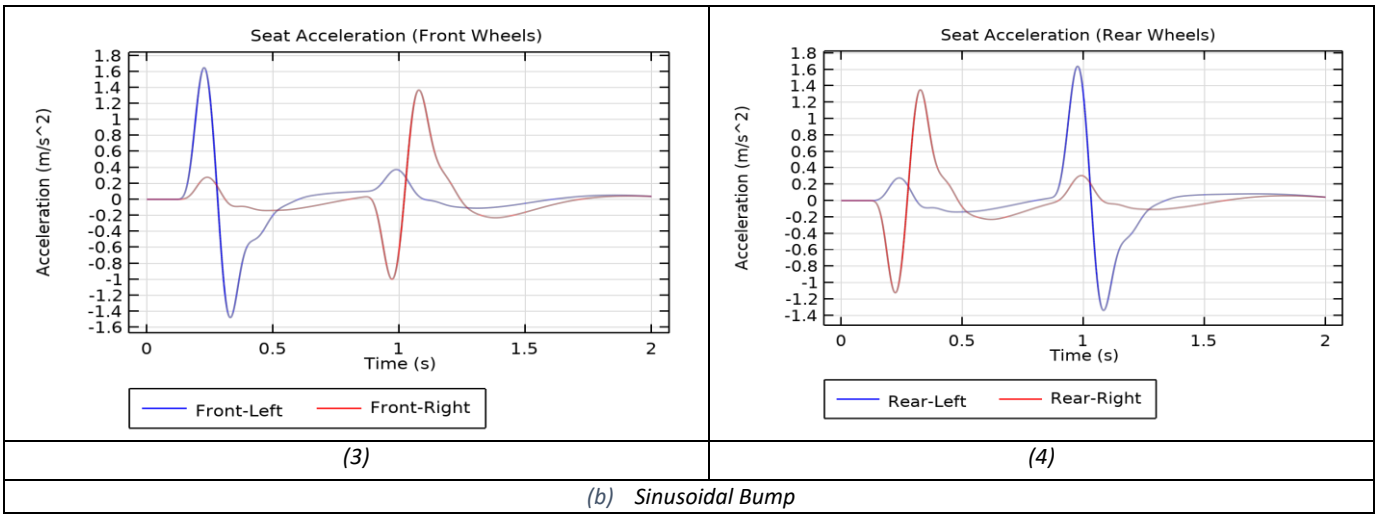

(3) (4)

(b) Sinusoidal Bump

Figure. 14 - Seat acceleration of the model at front wheels
(a) Rectangular Bump, (b) Sinusoidal Bump

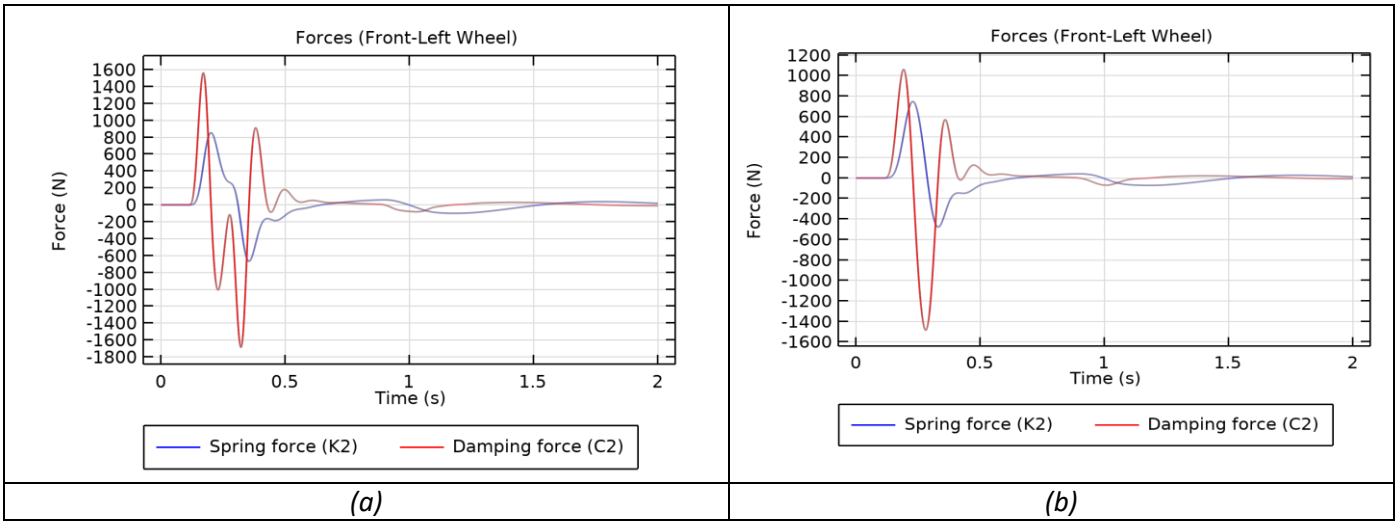

(a) (b)

Figure. 15 – Forces at the left wheel of the model
(a) Rectangular Bump, (b) Sinusoidal Bump

Journal of Engineering Research (JER)
ISSN: 2356-9441 Vol. 8 – No. 4, 2024 ©Tanta University, Faculty of Engineering e ISSN: 2735-4873

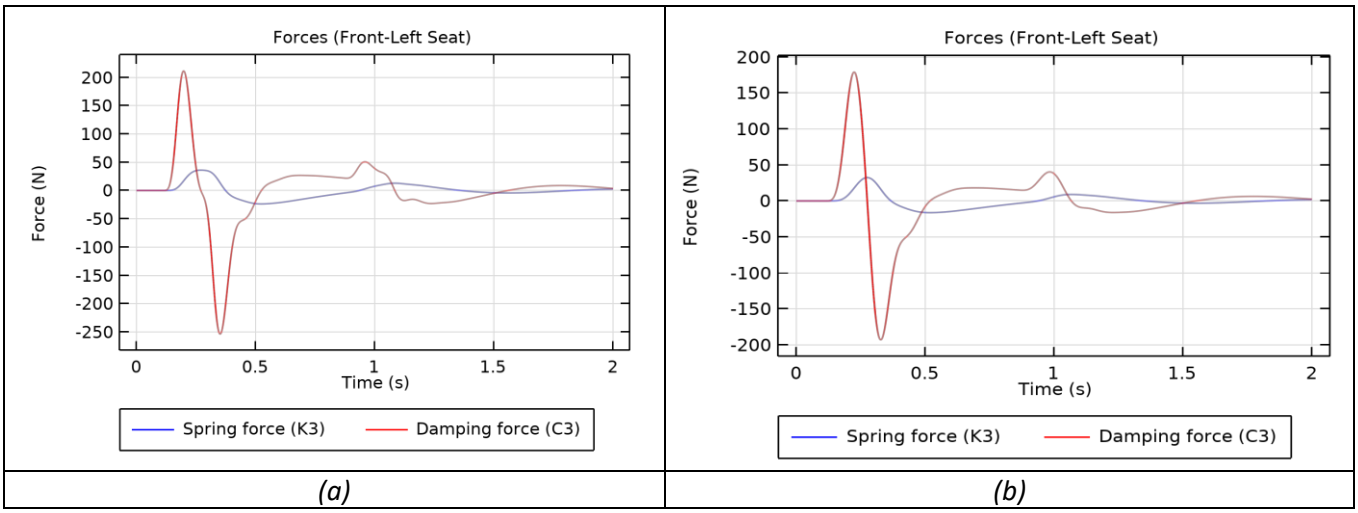

Figure. 16 - Forces at the left seat of the model
(a) Rectangular Bump, (b) Sinusoidal Bump

Figure. *16* presents the forces at the front seat on left side. The seat spring force varies periodically from -170 N to +230 N and the seat damping force is having peak of 22 N in case of rectangular bump. For the sine bump, the range of -180 N to +120 N is observed for seat spring force and the range of -20 N to +40 N.

A. Effect of single pulse road profile on vehicle performance

Figure. (17) shows that the amplitude and the frequency of excitation were kept equal in both cases for better comparison purpose. The peak amplitude of 0.5 deg of the rolling is observed for the rectangular bump whereas the peak of 0.4 deg is observed in the case of a sinusoidal bump about the roll axis. As only the left wheels of the vehicle pass over the bump, rolling happens from the left side to the right side of the vehicle and its nature is periodic. On the other hand, Figure. (18) presents the difference in rotation about the pitch axis shows a peak of 0.13 deg for a rectangular bump and 0.25 deg for a sinusoidal bump.

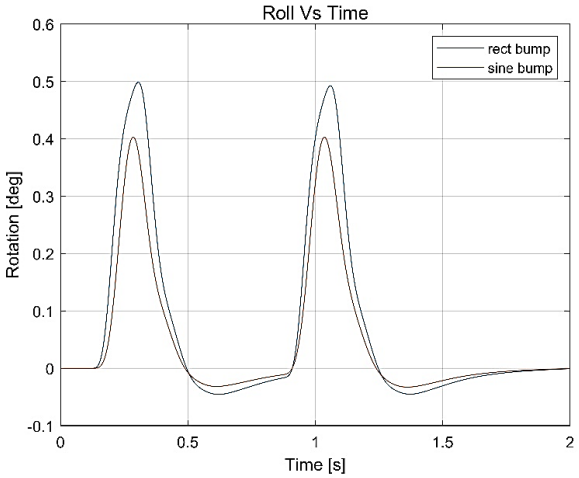

Figure. 17- comparison between rectangular and sinusoidal road profiles for roll degree

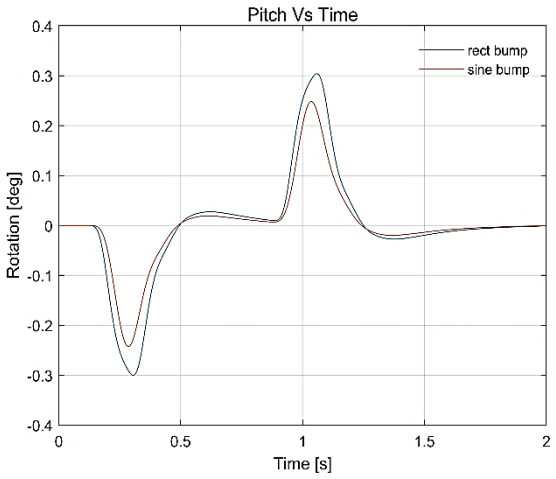

Figure. 18- comparison between rectangular and sinusoidal road profiles for rotation about pitch

Figure. (19) illustrates a peak of 8.5 mm observed in the case of rectangular bump whereas a peak of 5.6 mm is observed in the case of sine bump. Heave displacement shows a decreasing trend in amplitude over time, on the other hand, Figure. (20) shows the angular velocity of rolling with two significant peaks of equal amplitude of 0.105 rad/sec for rectangular bumps. A similar trend is observed for sinusoidal bumps with 0.09 rad/ for rolling velocity.

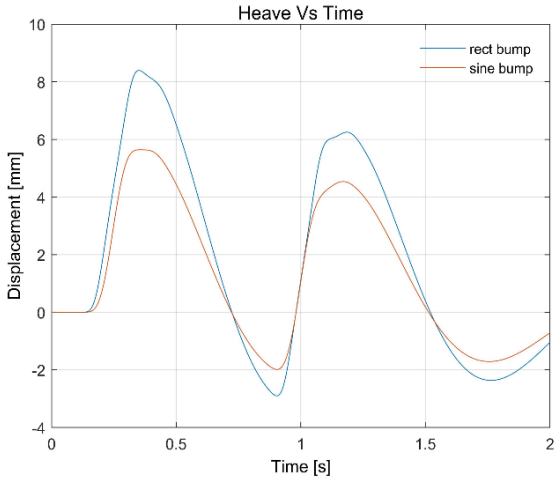

Figure.19- comparison between rectangular and sinusoidal road profiles for Displacement

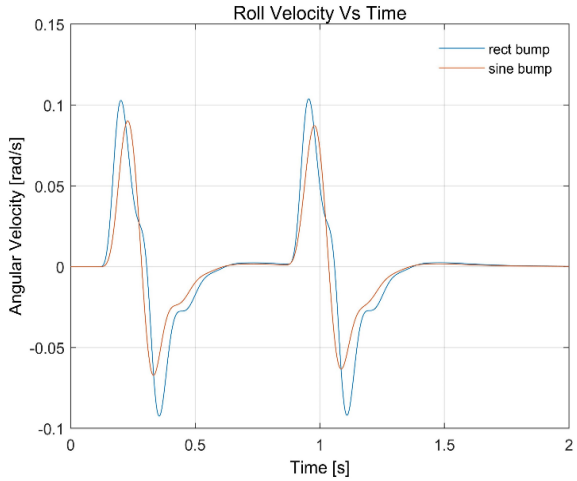

Figure. 20- comparison between rectangular and sinusoidal road profiles for angular velocity

Figure. (21) illustrates a peak value in pitching angular velocity for rectangular bump for a maximum value of 0.06 rad/s, while reaches a value of 0.05 rad/s for sinusoidal bump, comparing between the two road profiles according to the heave velocity, it can be observed that rectangular bump recorded a peak value of 0.06 m/s while the sinusoidal bump recorded a peak value 0.055 m/s as shown in Figure. (22).

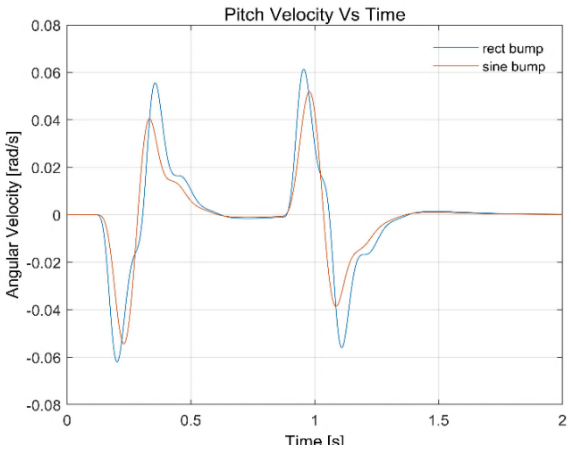

Figure.21- comparison between rectangular and sinusoidal road profiles for pitch angular velocity

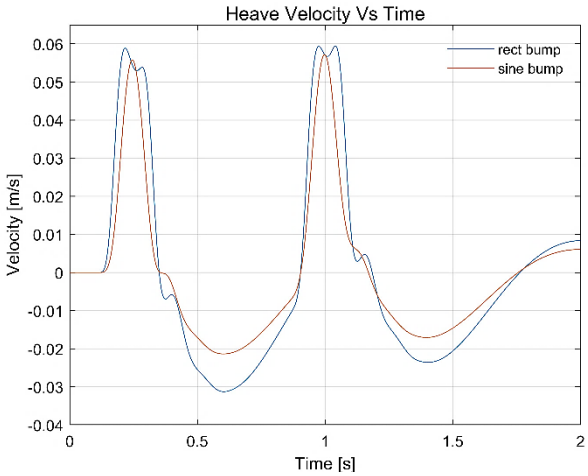

Figure.22- comparison between rectangular and sinusoidal road profiles for heave velocity

Journal of Engineering Research (JER)
ISSN: 2356-9441 Vol. 8 – No. 4, 2024 ©Tanta University, Faculty of Engineering e ISSN: 2735-4873

Figures 23,24 observes the time delay in seat displacement at the front and rear end, the seat displacements at the front and rear seats of the left side are significant in both cases, the peak displacement of 22 mm is observed at the front left seat for the rectangular bump whereas the displacement of 15.2 mm at the front left seat for the sine bump. Significantly smaller peak displacements are observed at the rear left seats for both types of bumps.

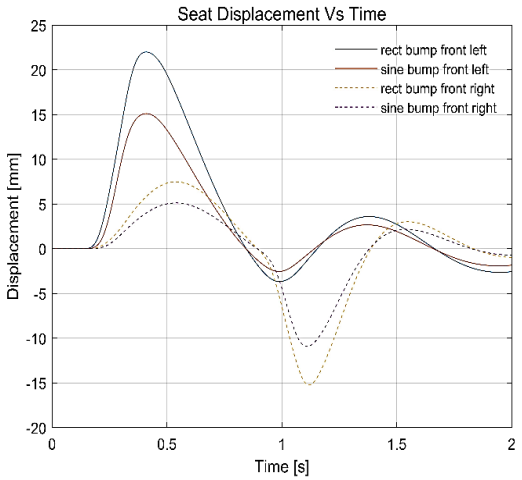

Figure.23- comparison between rectangular and sinusoidal road profiles for front seat displacement

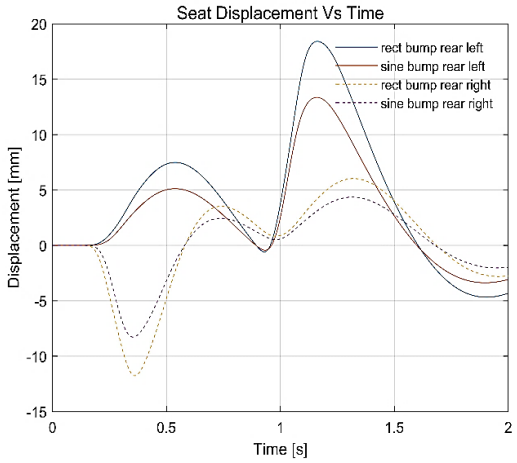

Figure.24- comparison between rectangular and sinusoidal road profiles for rear seat displacement

Figures 25,26 shows the left side seat with an acceleration range of around -2 to +2 m/s2 whereas the right side seat acceleration is noted as -1.25 to +1.75 m/s2 at the front wheels for rectangular bump. In the case of a sinusoidal bump, the left-side seat acceleration ranges from -1.5 to 1.62 m/s2, and right-side seat acceleration is noted from -1 to +1.4 m/s2 at the front wheels. Similar values are observed at the rear seat on both sides for rectangular as well as sine bump.

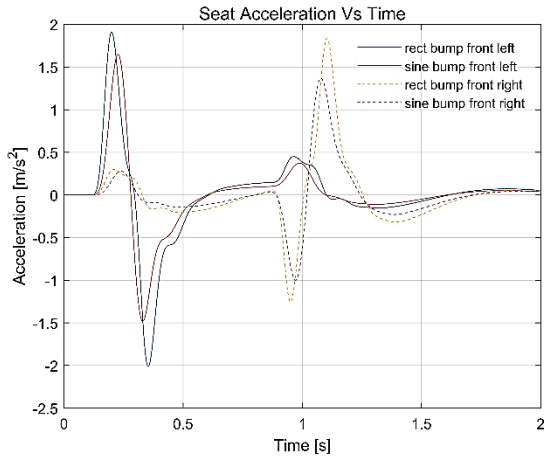

Figure.25- comparison between rectangular and sinusoidal road profiles for front seat acceleration

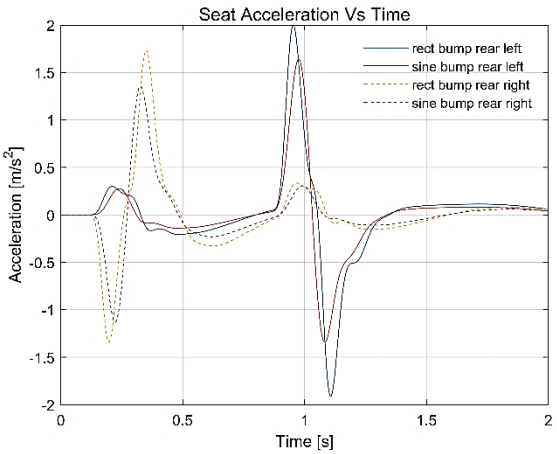

Figure.26- comparison between rectangular and sinusoidal road profiles for rear seat acceleration

Journal of Engineering Research (JER)
ISSN: 2356-9441 Vol. 8 – No. 4, 2024 ©Tanta University, Faculty of Engineering e ISSN: 2735-4873

Figures. 27,28 compares between the rectangular bump and sinusoidal bump for the suspension spring force varies periodically from -600 N to +800 N, whereas suspension damping force varies from –1600 N to +1600 N. On the other hand, the suspension spring force in the case of the sine bump is found to in range from -400 N to +750 N. The suspension damping force has the value of -1400N and +1050 N respectively.

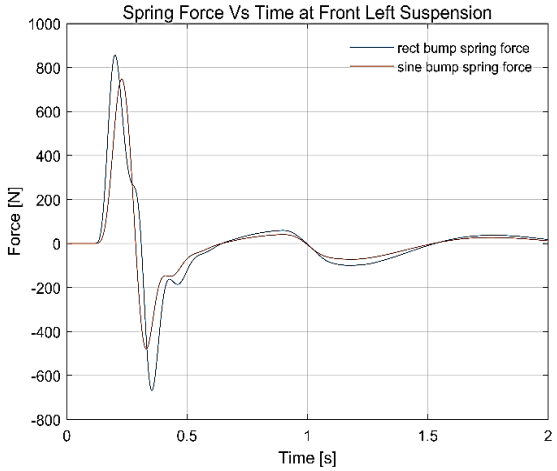

Figure.27- comparison between rectangular and sinusoidal road profiles for spring force at front left suspension

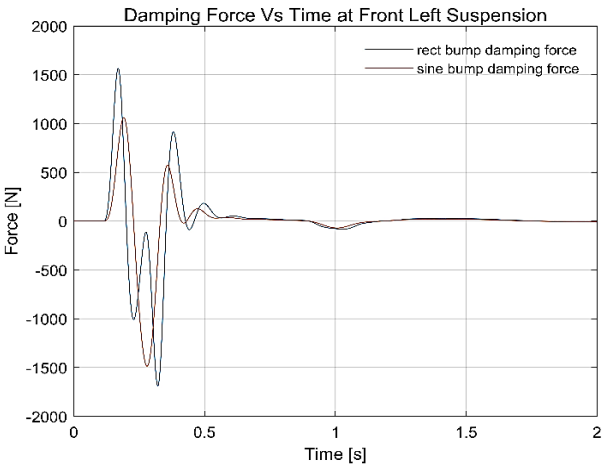

Figure.28- comparison between rectangular and sinusoidal road profiles for damping force at front left suspension

Figures. 29,30 compares between the rectangular bump and sinusoidal bump for the seat spring force which varies from -35 N to +35 N and the seat damping force has a peak of 220 N in case of a rectangular bump. While for the sine bump, the range of -20 N to +30 N is observed for seat spring force, and the range of -200 N to +170 N is noted for seat damping force.

It is important to note here that the effect of aerodynamic forces are neglected at such low speeds, as recommended by the experimental research previously conducted [13], which concluded that the dynamic simulation has the great effect on car performance at low cruise speeds. On the other hand, it is recommended for simulations at low cruise speeds below 36 km/hr where the deformation of mesh does not occur (no interaction) we can use the dynamic model simulation which can save time and effort, but for the other cruise speeds we must take in account the effect of aerodynamic forces with the presence of FSI model.

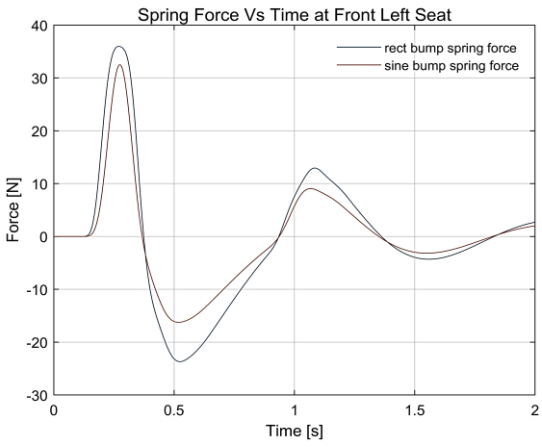

Figure.29- comparison between rectangular and sinusoidal road profiles for spring force at front left seat

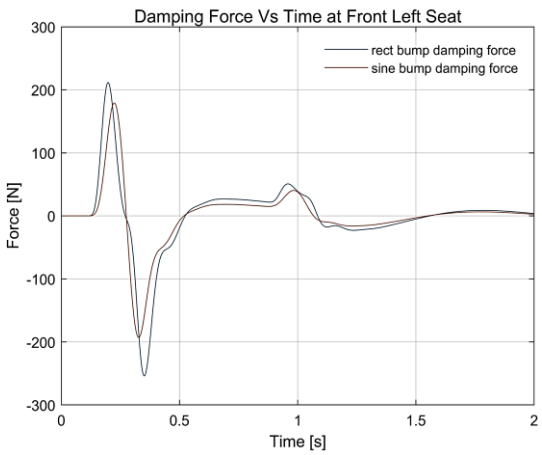

Figure.30- comparison between rectangular and sinusoidal road profiles for damping force at front left seat

Journal of Engineering Research (JER)
ISSN: 2356-9441 Vol. 8 – No. 4, 2024 ©Tanta University, Faculty of Engineering e ISSN: 2735-4873

B. Effect of continuous irregular road profiles on vehicle performance

The heave displacement around the centre of gravity is shown in Figure. 31. The peak of 9.6 mm is observed in case of rectangular bump whereas peak of 18.7 mm is observed in case of sine bump.

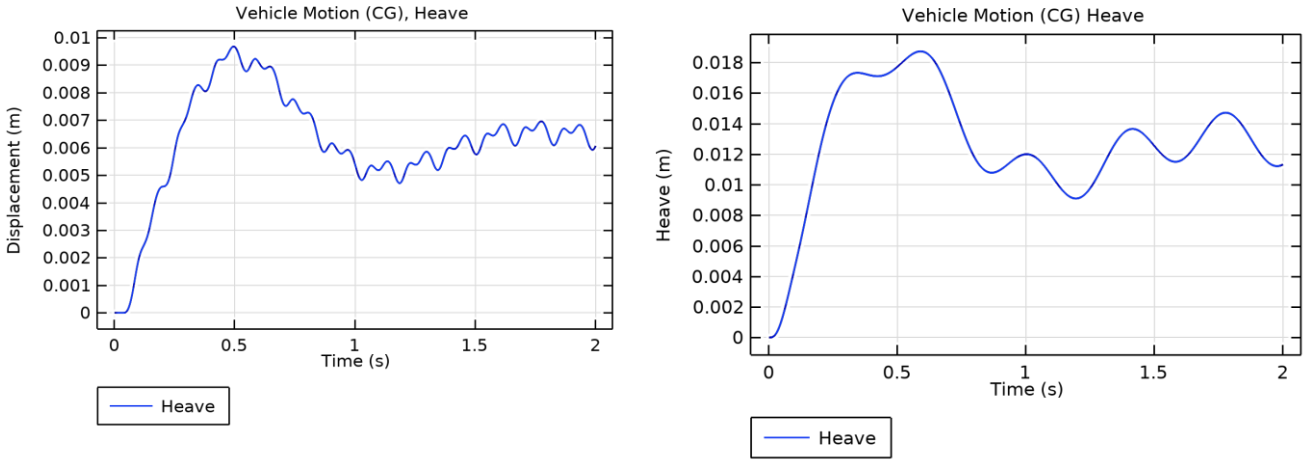

(a) *(b)*

Figure. 31 – Heave displacement at the centre of gravity
(a) continuous rectangular bump, (b) continuous sinusoidal bump

It is obvious to observe the time delay in seat displacement at the front and rear end. As only the left wheels are passing over the bump the displacement on the right side is negligible. The seat displacements at the front and rear end of the left side are significant. Initially, the displacement increases up to 0.7 sec and then starts reducing harmonically. The peak of 19.2 mm is observed in the case of the rectangular bump whereas the peak of 40 mm is seen for the sine bump.

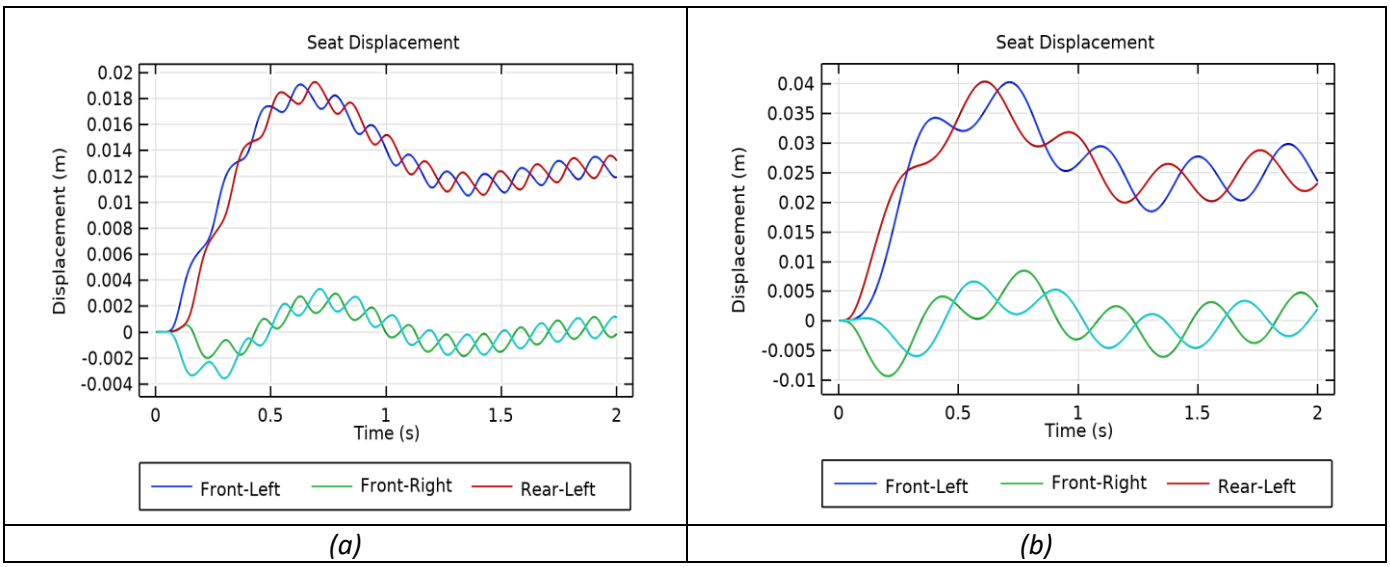

(a) *(b)*

Figure. 32- Seat displacement of the model
(a) continuous rectangular bump, (b) continuous sinusoidal bump

The spring forces and damping forces at the front left wheelbase are shown in Figure. 15. For rectangular bump, suspension spring force varies periodically from -3000 N to +2000 N, whereas suspension damping force varies from -550 N to +900 N. On the other hand, the suspension spring force in case of sine bump is found to be ranging from -520 N to +410 N. The suspension damping force have the value of -570N and +550 N respectively.

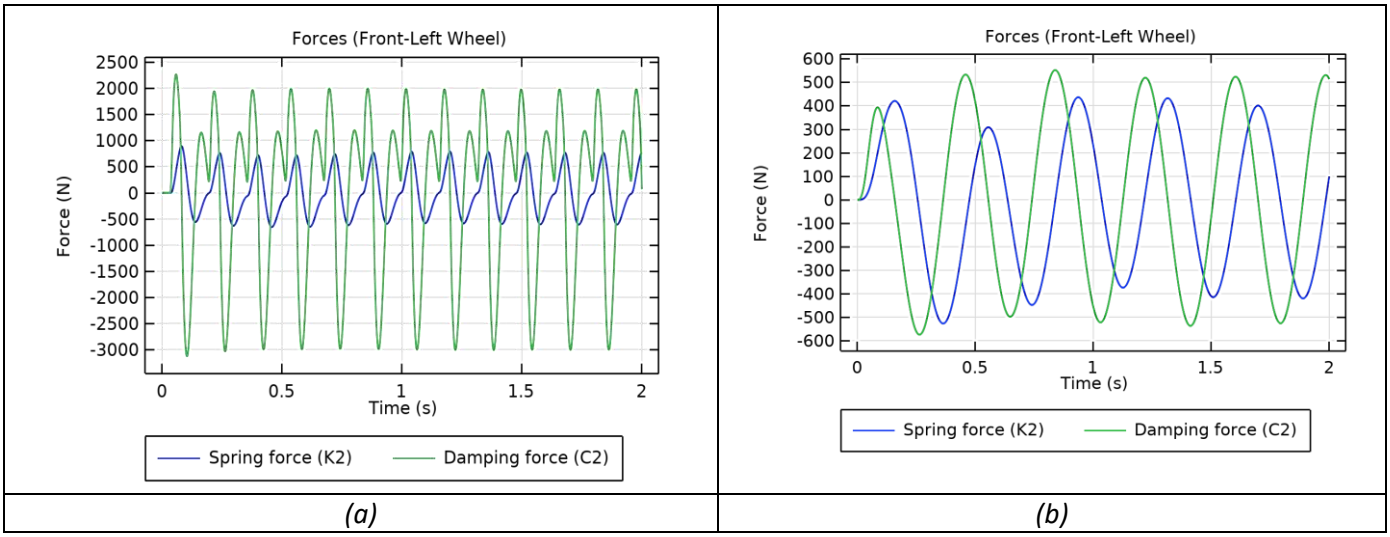

Figure. 32 – Forces at the left wheel of the model
(a) continuous rectangular bump, (b) continuous sinusoidal bump.

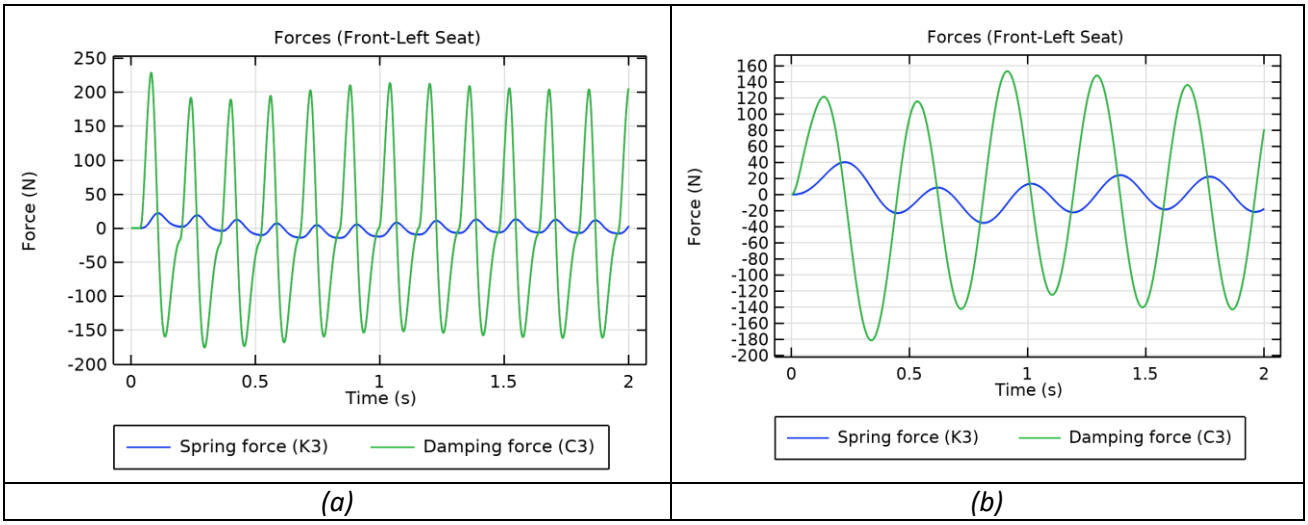

Figure. 33 – Forces at the left seat of the model
(a) continuous rectangular bump, (b) continuous sinusoidal bump

Figure. (34) shows the comparison between the effect of two different road profiles on the jerk function of the car seat which is calculated from the derivation of the seat acceleration when passing over single road bump, which gives an overview of the passenger comfort. From the Figure. it can be concluded that for rectangular bump the seat acceleration, jerk function records higher values than the sinusoidal road profile.

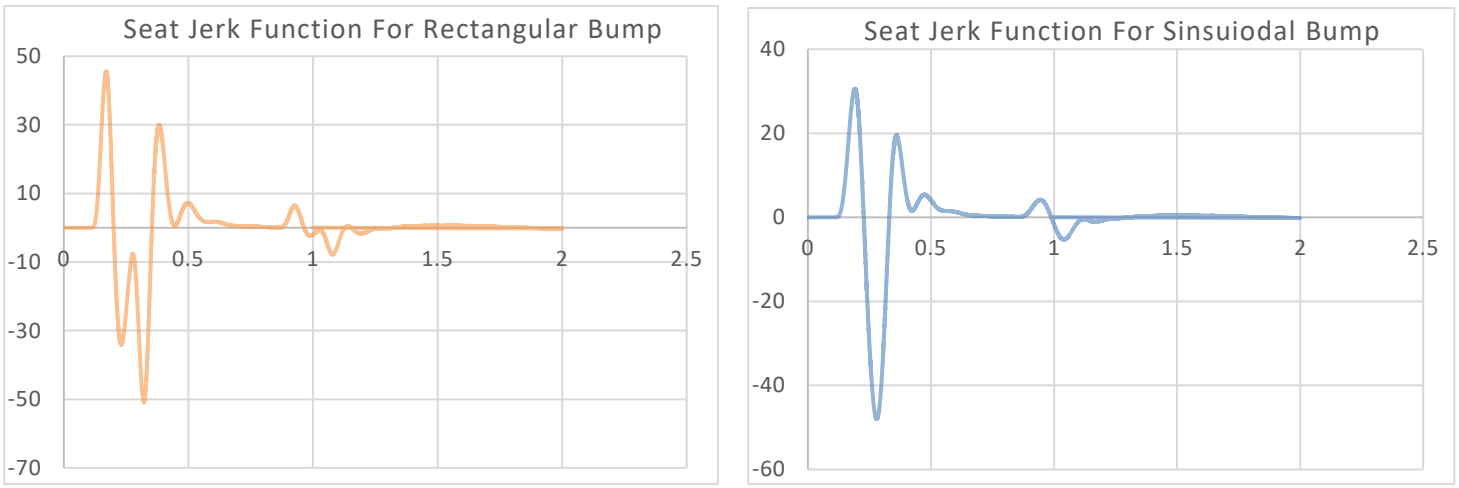

Figure. 34- comparison between rectangular and sinusoidal single bump for jerk function.

The values resulted from simulation shows that the maximum value of acceleration in rectangular Bump of 1.914 m/s2, the maximum value of acceleration in sinusoidal bump 1.649 m/s2, the maximum value of jerk in rectangular bump = 45.5 m/s3, the maximum value of jerk in sinusoidal bump= 30.6 m/s3. On the other hand, the maximum value of acceleration in continuous sinusoidal bump=1.2534 m/s2, the maximum value of jerk in continuous sinusoidal bump= 20.216 m/s3, the maximum value of acceleration in continuous rectangular bump=2.009 m/s2, the maximum Value of jerk in continuous Rectangular Bump=65.76 m/s3.

Table 3 shows a comparison between the maximum value of acceleration and the maximum value of jerk in rectangular bump and sinusoidal bump in case of single and continuous bumps.

Road profile type	Single Bump		Continuous bump	
	Acceleration m/s^2	Amount of Jerk m/s^3	Acceleration m/s^2	Amount of Jerk m/s^3
rectangular Bump	1.914	45.5	1.2534	20.216
sinusoidal bump	1.649	30.6	2.009	65.76

According to the standard values of comfort in ISO 2631 [14], it can be concluded that discomfort increases in an approximately linear fashion with acceleration magnitude, and acceleration is the most important predictor of comfort. The accelerations up to 0.28 m/s2 feel 'Excellent'; and accelerations above 2.12 m/s2 feel 'Terrible'. The average 'So-so' point, which may be interpreted as a threshold for acceptable acceleration, was 1.23 m/s2. On average, the effect of jerk appears to be negative, meaning that higher jerks are associated with less discomfort. This observation appears counterintuitive when we consider jerk analogous to the experience of a 'kick'. However, higher jerks also meant shorter duration pulses, such that the highest jerks were experienced for the shortest pulses. And jerk was limited to 15 m/s3.

III. CONCLUSION AND FUTURE WORK

In this work, a methodology was developed to design a passive suspension for a passenger car using a full car model in lumped mechanical system interface of COMSOL Multiphysics. This simulation model is used as a platform to analyse the performance of vehicle dynamics and ride comfort for different standard road profiles with accordance to ISO 2631-1. From the results obtained from simulation it can be concluded that:

1- The displacement of car C.G. under rectangular road bump profile is 29% higher than in sinusoidal road profile. The pitch angular velocity in case of rectangular road profile has also 16.7% higher than sinusoidal road profile.
2- According to the front left seat displacement, the rectangular road profile has 44.7% higher value than the sinusoidal road profile. On the other hand, the front left seat acceleration analysis shows that rectangular road profile is 16.67% higher than sinusoidal road profile. Both values recorded as uncomfortable in accordance to the ISO standard.
3- Considering the jerk function, it can be concluded that the maximum value of jerk in rectangular bump recorded values 48.7% higher than sinusoidal bump. Both values are also on the uncomfortable zone according to the ISO standard.
4- In continuous irregular road profile, the values recorded for rectangular bump are lower in single bump both acceleration and jerk. But in case of sinusoidal bumps extreme values of acceleration and jerk are recorded which are considered as terrible in accordance to the ISO standard.

Conflicts of Interest: The authors declare no conflict of interest.

REFERENCES

1- Fayyad, Sayel M. "Constructing control system for active suspension system." Contemporary Engineering Sciences 5, no. 4 (2012): 189-200.
2- Valášek, Michael, and Willi Kortüm. "Semi-active suspension systems II." In The Mechanical Systems Design Handbook, pp. 221-238. CRC Press, 2017.
3- El-Gohary, M. A., B. M. El-Souhily, S. F. Rezeka, and T. Awad. "Generalized Model for Front-Wheel Mid-Size Passenger Car." Eur. J. Sci. Res 52 (2011): 413-429.
5- Yaghoubi, Saeed, and Afshin Ghanbarzadeh. "Modeling and optimization of car suspension system in the presence of magnetorheological damper using Simulink-PSO hybrid technique." Results in Engineering 22 (2024): 102065.
6- El-Kafafy, Mahmoud, Samir M. El-Demerdash, and Al-Adl Mohamed Rabeih. "Automotive ride comfort control using MR fluid damper." (2012).
7- Batistini, Leonardo, Serena Donati, Matteo Nori, Lorenzo Tirabassi, Francesco Bucchi, and Francesco Frendo. "Suspension and tyre loads estimation of an FSAE car: model development and on-track validation." Vehicle System Dynamics (2024): 1-22.
8- Kumar, Jitender, and Gian Bhushan. "Dynamic analysis of quarter car model with semi-active suspension based on combination of magneto-rheological materials." International Journal of Dynamics and Control 11, no. 2 (2023): 482-490.
9- Geweda, A. E., M. A. El-Gohary, A. M. El-Nabawy, and T. Awad. "Improvement of vehicle ride comfort using genetic algorithm optimization and PI controller." Alexandria Engineering Journal 56, no. 4 (2017): 405-414.
10- Nagarkar, Mahesh P., M. A. El-Gohary, Yogesh J. Bhalerao, Gahininath J. Vikhe Patil, and Rahul N. Zaware Patil. "Artificial neural network predication and validation of optimum suspension parameters of a passive suspension system." SN Applied Sciences 1, no. 6 (2019): 569.
11- Yakhni, Mohammad Faisal, Mohamad Ali, and Mohamed El-Gohary. "CONTROL OF MR DAMPER USING ANFIS AND PID CONTROLLER FOR OPTIMUM VEHICLE RIDE COMFORT." BAU Journal-Science and Technology 2, no. 1 (2020): 10.
12- Abd_Elsalam, A., M. A. El-Gohary, and H. A. El-Gamal. "Simulation of nonlinear quarter car suspension system with and without tire damping." International Journal of Advanced Scientific and Technical Research 6, no. 6 (2016): 98-105.
13- Abidin, Ahmad Noor Syukri Zainal, Arief Hakimi Azmi, Azzuhana Roslan, Roziana Shahril, Ahmad Shahir Jamaludin, Nur Aini Safiah binti Abdullah, Zulhaidi Mohd Jawi, and Khairil Anwar Abu Kassim. "ASEAN 3-5-2 in Road Crash Data Management: Turning Midfields into Forward." Journal of Advanced Vehicle System 13, no. 2 (2022): 31-37.
14- Zakher Bassem Nashaat, Mostafa El-Hadary, Mohammed Abd Elfatah Elgohary, and Ibrahim M. El Fahham. "A Comparison Between Experimental Life Road Simulation and Computational Fluid Dynamics and Fluid Structure Interaction for Sedan Car." CFD Letters 14, no. 2 (2022): 81-97.
15- De Winkel, Ksander N., Tugrul Irmak, Riender Happee, and Barys Shyrokau. "Standards for passenger comfort in automated vehicles: Acceleration and jerk." Applied Ergonomics 106 (2023): 103881.
16- Güçlü, Rahmi. "Active control of seat vibrations of a vehicle model using various suspension alternatives." Turkish Journal of Engineering and Environmental Sciences 27, no. 6 (2003): 361-374.
17- Zakher Bassem Nashaat, Mostafa El-Hadary, and Andrew Nabil Aziz. "The Effect of Vortex Generators on Aerodynamics for Sedan Cars." CFD Letters 11, no. 6 (2019): 1-17.
18- Zakher B., and Dalia M. Ammar. "The effect of changing the slant angle of Ahmeds car model on drag coefficient for different cruise speeds." J Recent Trends Mech (2019). http://doi.org/10.5281/zenodo.2637879.
19- COMSOL Multiphysics Modeling Guide, by COMSOL AB. 2023.